Published in final edited form as:

Nature. 2019 March ; 567(7746): 105–108. doi:10.1038/s41586-019-0936-6.

Female-biased embryonic death from genomic instability-induced inflammation

Adrian J. McNairn[1], **Chen-Hua Chuang**[2], **Jordana C. Bloom**[1], **Marsha D. Wallace**[3], and **John C. Schimenti**[1,4,*]

[1]Cornell University College of Veterinary Medicine, Dept. of Biomedical Sciences

[2]AbbVie Inc, Redwood City, CA

[3]University of Oxford.

[4]Cornell Center for Vertebrate Genomics.

Abstract

Genomic instability (GIN) can trigger cellular responses including checkpoint activation, senescence, and inflammation [1,2]. Though extensively studied in cell culture and cancer paradigms, little is known about the impact of GIN during embryonic development, a period of rapid cellular proliferation. We report that GIN-causing mutations in the MCM2–7 DNA replicative helicase [3,4] render female mouse embryos to be dramatically more susceptible than males to embryonic lethality. This bias was not attributable to X-inactivation defects, differential replication licensing, or X vs Y chromosome size, but rather "maleness," since XX embryos could be rescued by transgene-mediated sex reversal or testosterone (T) administration. The ability of exogenous or endogenous T to protect embryos was related to its anti-inflammatory properties [5]. The NSAID ibuprofen rescued female embryos containing mutations not only in MCM genes but also *Fancm,* which like MCM mutants have elevated GIN (micronuclei) from compromised replication fork repair [6]. Additionally, deficiency for the anti-inflammatory IL10 receptor was synthetically lethal with the *Mcm4*^{Chaos3} helicase mutant. Our experiments indicate that DNA replication-associated DNA damage during development induces inflammation that is preferentially lethal to female embryos, whereas male embryos are protected by high levels of intrinsic T.

Mutations that compromise DNA replication or replication-associated repair can cause replication stress (RS) and GIN [7,8]. Resulting chronic DNA damage can lead to inflammation by activating the cGAS/STING pathway, potentially resulting in a

[*]**Corresponding author.** All correspondence and requests for reagents or permissions should be directed to John Schimenti. jcs92@cornell.edu.

Author Contributions. C-H. C. made the original observations of sex skewing and performed studies with T and the *Sry* transgene while at Cornell University. A.M. discovered the link to inflammation and also the effect of maternal genotype, and performed all those related experiments; he also helped write and assemble the manuscript. M.W. performed the X inactivation study. J.B. developed the *Fancm* mice and analyzed sex ratios. J.S. supervised all aspects of the work and wrote the manuscript.

Competing interests. The authors declare no competing interests.

"senescence-associated secretory phenotype" (SASP) [1,9,10]. Little is known about consequences of fetal or maternal GIN-induced inflammation during gestation.

DNA replication requires the heterohexameric minichromosome maintenance complex (MCM2–7), constituting the catalytic core of the replicative helicase. Reduction of MCMs causes RS by decreasing dormant ("backup") origins that are important for completing DNA replication when replication forks stall or collapse [11–13]. Mice bearing the *Chaos3* allele of *Mcm4* (abbreviated $Mcm4^{C3}$) have elevated micronuclei and are highly cancer prone [4]. This allele causes GIN by destabilizing the MCM2–7 helicase and triggering post-transcriptional pan-reduction (~40%) of *Mcm2–7* mRNAs and protein [3]. Although $Mcm4^{C3}$ homozygotes in strain C3H are fully viable, compound heterozygosity for certain other *Mcm* genes causes severe phenotypic consequences including pre- and postnatal lethality [3]. Upon closer examination of those and additional breeding data, we noticed that females of the MCM-depleted, semi-lethal genotypes $Mcm4^{C3/Gt}$, $Mcm4^{C3/C3}$ $Mcm2^{Gt/+}$, $Mcm4^{C3/C3}$ $Mcm6^{Gt/+}$, and $Mcm4^{C3/C3}$ $Mcm7^{Gt/+}$ (Gt = gene trap allele) were drastically under-represented compared to males of the same mutant genotype (Fig. 1a; Tables S1, S2, S3, S4). There was no gender skewing associated with non-lethal genotypes ($Mcm4^{C3/C3}$ $Mcm3^{Gt/+}$ and $Mcm4^{C3/C3}$ $Mcm5^{Gt/+}$), i.e., those genotypes present in offspring at Mendelian ratios (Fig. 1a; Table S5) [3].

To determine when $Mcm4^{C3/C3}$ $Mcm2^{Gt/+}$ females were dying during development, we conducted timed matings of $Mcm4^{C3/C3}$ females to $Mcm4^{C3/+}$ $Mcm2^{Gt/+}$ males. Loss of $Mcm4^{C3/C3}$ $Mcm2^{Gt/+}$ embryos was first evident at E14.5, and was already skewed against females; the male:female ratios of $Mcm4^{C3/C3}$ $Mcm2^{Gt/+}$ embryos at E9.5, E12.5, E14.5 and birth were 1.0, 1.37, 2.0, and 3.11, respectively (Fig. 1b).

MEFs (mouse embryonic fibroblasts) bearing MCM mutations exhibit reduced dormant replication origins [14,15]. To test if dormant origin reduction contributes to the female-biased lethality, *Mcm3* heterozygosity was introduced into the semilethal genotypes. *Mcm3* heterozygosity ameliorates several deleterious phenotypes of MCM-deficient mutant mice and cells by increasing chromatin-bound MCMs (MCM3 participates in nuclear export of MCMs) [3]. This dramatically rescued viability of $Mcm4^{C3/Gt}$ and $Mcm4^{C3/C3}$ $Mcm6^{Gt/+}$ female embryos preferentially, increasing female viability from 0% to 27% in the former, and from 3% to 42% in the latter (Fig. 1a, Tables S1,S2). *Mcm3* heterozygosity also increased viability of $Mcm4^{C3/C3}$ $Mcm2^{Gt/+}$ newborns from 30% to 72%, but both sexes were rescued approximately proportionately (Fig. 1a; Table S3); preferential female rescue may be related to overall degree of lethality in compound mutants (93%, 82% and 70% lethality for $Mcm4^{C3/Gt}$, $Mcm4^{C3/C3}$ $Mcm6^{Gt/+}$ and $Mcm4^{C3/C3}$ $Mcm2^{Gt/+}$, respectively) [3].

We next hypothesized that the female-biased embryonic lethality was related to one of the following: 1) defects in X-inactivation caused by impaired or delayed DNA replication, 2) the larger size of the X (~171 Mb) vs the Y chromosome (~90 Mb), which might stress the compromised replication machinery, or 3) secondary sexual characteristics. Flow cytometric analysis of cells from E10.5 female embryos bearing an ubiquitously-expressed X-linked GFP transgene revealed no difference between non-lethal genotypes ($Mcm4^{C3/+}$ $Mcm2^{Gt/+}$; $Mcm4^{C3/+}$ $Mcm2^{+/+}$; $Mcm4^{C3/C3}$ $Mcm2^{+/+}$) and the sex-biased lethal genotype ($Mcm4^{C3/C3}$

Mcm2$^{Gt/+}$; Extended Data Fig. 1), indicating that X-inactivation occurs normally. To distinguish between hypotheses 2 and 3, a single experiment was performed. We induced sex reversal of XX *Mcm4*$^{C3/C3}$ *Mcm2*$^{Gt/+}$ embryos with an autosomal *Sry* transgene. Strikingly, this increased the proportion of XX *Mcm4*$^{C3/C3}$ *Mcm2*$^{Gt/+}$ mice from 20% to 48% (Fig 2a; Table S6). These results indicate that maleness, and not the presence of two X chromosomes *per se*, protects embryos from MCM deficiency. These data are consistent with the finding that preferential female embryo death occurs after sex determination (E9.5–12.5).

Since sex reversal rescued XX lethality, we hypothesized that testosterone (T) might be responsible. It is produced at high levels by Leydig cells in embryonic testes from ~E12.5 onward [16]. We injected pregnant females daily with T beginning at E7.5, and found that the viability of XX *Mcm4*$^{C3/C3}$ *Mcm2*$^{Gt/+}$ E19.5 fetuses increased dramatically from 22% to 54% (Fig. 2a; Table S7). We speculated that T might protect MCM-deficient embryos by increasing replication capacity, given a report that the androgen receptor stimulates proliferation of prostate cancer cells by acting as a replication factor [17,18]. However, we observed no increase of *Mcm* mRNA or chromatin-bound MCMs in T-treated MEFs (Fig. 2b, c), and no sex-specific differences in MCM2 or MCM4 protein levels in E13.5 fetuses or placentae of various genotypes (Extended Data Fig. 2).

Next, we hypothesized that T was ameliorating certain consequences of GIN in the *Mcm* mutants. In particular, elevated micronuclei, the signature phenotype of *Mcm4*^{Chaos3} mice [4], can trigger inflammation via the cGAS-STING pathway [19]. T, a steroid hormone, suppresses the expression of pro-inflammatory cytokines while increasing the anti-inflammatory molecule IL10 [5,20,21]. Indeed, T treatment of *Mcm4*$^{C3/C3}$ *Mcm2*$^{Gt/+}$ MEFs caused >2–3 fold decreases in mRNAs for the pro-inflammatory cytokine IL6 and also PTGS2 (COX2), which is central for production of prostaglandins that cause inflammation and pain (Fig. 2b). Strikingly, administration of ibuprofen to pregnant females (from 7.5 days post-coitus onward in drinking water) completely abolished sex bias of *Mcm4*$^{C3/C3}$ *Mcm2*$^{Gt/+}$ offspring (Fig. 2a, Extended Data Table 1a) without affecting embryonic or placental MCM levels (Extended Data Fig. 2b, c).

While these data indicate that GIN-driven inflammation underlies preferential female embryonic lethality, we considered the possibility that unrelated alterations in gene expression by ibuprofen and the androgen receptor (which is strongly induced by T; Fig. 2c) [22,23] were responsible. We therefore took the orthogonal approach of increasing inflammation by ablating the receptor (*Il10rb*) for the anti-inflammatory molecule IL10, hypothesizing that this would exacerbate *Mcm4*$^{C3/C3}$ *Mcm2*$^{+/-}$ lethality or sex bias. Remarkably, the genotype of *Mcm4*$^{C3/C3}$ *Il10rb*$^{-/-}$ caused highly penetrant lethality to embryos of both sexes (Extended Data Table 1c). IL10 mediates a feedback loop under conditions of inflammation to induce degradation of *Ptgs2*/*COX2* transcripts [24], and also counters the inflammation response triggered by the STING pathway [25]. This synthetic lethality was rescued by treating pregnant dams with NSAID, increasing viability of *Mcm4*$^{C3/C3}$*Il10rb*$^{-/-}$ offspring (both sexes) from 8.9% to 94% (Extended Data Table 1c).

Successful pregnancy requires suppression of inflammation at the maternal:fetal interface. Because homozygosity for *Chaos3* alone causes a ~20 fold increase in micronucleated

erythrocytes without decreasing viability in the C3H background[4], and IL10 is thought to play a role in suppressing maternal inflammation at the fetal:maternal interface [26], we speculated that maternal genotype might influence viability of MCM compound mutant embryos. We mated females heterozygous for *Chaos3* (*Mcm4*$^{C3/+}$ *Mcm2*$^{Gt/+}$) to *Mcm4*$^{C3/C3}$ males (all data presented heretofore were from reciprocal crosses). Surprisingly, this cross abolished the sex bias against *Mcm4*$^{C3/C3}$ *Mcm2*$^{Gt/+}$ females (Fig. 3a; Extended Data Table 1b). We hypothesized that maternal homozygosity for *Chaos3* imposes additional stress on the placentae of genetically susceptible female embryos, possibly via DNA damage-induced inflammation. We examined double strand break (DSB) levels (marked by γH2AX) in placentae of E13.5 embryos produced in various control and mutant reciprocal crosses. Regardless of fetal genotype, placentae from embryos within *Mcm4*$^{C3/C3}$ dams had more γH2AX-positive cells than when dams were of any other genotype (Fig. 4). NSAID treatment did not reduce the level of γH2AX staining, consistent with the rescue effect being related to inflammation, not GIN *per se* (Fig. 4). We therefore hypothesized that GIN-induced placental inflammation might underlie the lethality in our mice. Consistent with this, we observed significant reductions in placental, but not embryonic MCM2 and MCM4 (especially MCM4) in *Chaos3* mutant genotypes, regardless of maternal genotype or whether the dams were NSAID-treated (Extended Data Fig. 2a-c). Thus, placental cells may be particularly sensitive to DNA replication defects that trigger downregulation of MCM production and consequent increases in GIN and inflammation [27,28]. RNA-seq analysis of male vs female placentae from either *Mcm4*$^{C3/+}$*Mcm2*$^{Gt/+}$ or *Mcm4*$^{C3/C3}$ dams revealed increased expression of hallmark inflammation gene sets only in the lethal genotype combination of *Mcm4*$^{C3/C3}$ *Mcm2*$^{Gt/+}$ females from *Mcm4*$^{C3/C3}$ dams (Fig. 3b; Extended Data Fig. 3). The major upregulated gene sets included EMT transition (commonly associated with inflammatory responses [29]), allograft rejection, and interferon gamma response. All three of these categories contain genes involved in inflammation and the innate immune response (Extended Data Fig. 3). Overall, the results indicate that the combination of maternal and fetal GIN causes lethal levels of inflammation. However, it remains possible that the parental genotype-dependent, sex biased lethality may have an epigenetic component (i.e. imprinting).

While the data presented thus far demonstrate that MCM depletion (e.g. *Mcm2* hemizygosity) in conjunction with a destabilized replicative helicase in *Chaos3* mice trigger inflammation and embryonic death, it is unclear exactly what defects are primarily responsible, and whether the sex-bias phenomena are entirely unique to these models. We therefore attempted to parse the key proximal defects that trigger the sex bias by exposing WT embryos to either exogenous RS alone or DSBs alone. Pregnant females, treated with hydroxyurea to induce RS, delivered pups without significant sex skewing (M:F 1.08; Table S8). Chronic exposure to ionizing radiation, which causes DSBs, also failed to produce a sex bias (M:F 1.00; Table S8). We then conjectured that replication-associated DNA damage that causes micronuclei might underlie the inflammation-driven lethality. Mice deficient for FANCM, involved in DNA replication fork repair, display elevated micronuclei [6] and underrepresentation of females [30]. We also observed a bias against *Fancm*$^{-/-}$ females in heterozygote crosses (M:F 1.68; χ^2 p = 0.03; Fig 1a, Extended Data Table 1d) that was

rescued by ibuprofen treatment of dams (*Fancm*$^{-/-}$ M:F 1.13 vs *Fancm*$^{+/+}$ 1.07; Fig. 2a, Extended Data Table 1d).

Our results indicate that DNA damage caused by defective DNA replication and/or replication-associated repair cause a level of inflammation compromising female embryos lacking anti-inflammatory protection of testosterone. We hypothesize that since both genetic models tested have elevated micronuclei, a known trigger of the cGAS-STING cytosolic DNA sensing pathway, that this may precipitate lethal inflammation in a key compartment(s) of the embryo and/or uterine environment. Future experiments exploiting mouse mutants and mosaics will help resolve these questions, and guide studies into whether similar phenomena occur in humans.

Methods

Mice.

All breeding and husbandry all crosses were performed in the same animal facility and room at Cornell's Veterinary College (East Campus Research Facility), and under the same environmental conditions and health status. Use of mice was performed in compliance with all relevant ethical regulations, having been conducted under a protocol (0038–2004) approved by Cornell University's Institutional Animal Care and Use Committee (IACUC). Sample sizes for original sex skewing observations, since they were taken from historical colony breeding data, were not planned, and selection of individuals was entirely genotype-based, thus not randomized. Sexing of animals was done before genotyping, thus there was no blinding. Sample sizes with T and ibuprofen were also not pre-determined, as potential effect size was unknown yet proved to be dramatic.

Testosterone Injections and Sex Reversal.

Mcm4$^{C3/C3}$ *Mcm2*$^{Gt/+}$ males were mated to *Mcm4*$^{C3/C3}$ females and 100uL of a 3mg/ml solution of testosterone propionate (Sigma) was injected sub-cutaneously into the hind leg of pregnant females daily from E7.5 to E.16.5 (20μg/g/day). This dose has been shown to increase female fetal testosterone by 80% in a rodent model without serious toxicological effect [31]. The testosterone propionate was dissolved in corn oil and filter sterilized prior to injection. MEFs were derived from E13.5 embryos using *Mcm4*$^{C3/C3}$ *Mcm2*$^{Gt/+}$ males mated to *Mcm4*$^{C3/C3}$ females. MEFs were genotyped and treated with Plasmocin (InvivoGen) to prevent mycoplasma. For treatment of MEFs, a 50mM solution of testosterone propionate was prepared in ethanol and cells were treated with 10nM for 1 hour. The media was then removed and the cells collected at indicated timepoints. Sex reversal of *XX Mcm4*$^{C3/C3}$ *Mcm2*$^{Gt/+}$ embryos was carried out using an autosomally-linked *Sry* transgene (Tg(*Sry129)4Ei*) [32].

Ibuprofen Treatment.

Mcm4$^{C3/C3}$ *Mcm2*$^{Gt/+}$ males were mated to *Mcm4*$^{C3/C3}$ females and at E7.5-E9.5 the pregnant females were provided with water bottles containing ibuprofen (Children's Advil) 5mL(100mg) in 250mL. They were allowed to drink ad libitum (50–80mg/kg/day). Newborns were genotyped at birth for sex with *Sry* primers and *Mcm* mutation status.

Control mice utilized the same male with another *Mcm4*$^{C3/C3}$ female and no drug treatment. For *Il10rb*, the strain was obtained from Jax Mice (stock#005027) and backcrossed into the C3Heb/FeJ (Jax stock#000658) background for six generations (N6) before crossing into the *Mcm4*^{C3} strain for 2 additional generations (N2). *Mcm4*$^{C3/C3}$*Il10rb*$^{+/-}$ males were mated to *Mcm4*$^{C3/C3}$*Il10rb*$^{+/-}$ females and provided with ibuprofen as described above. Newborns were genotyped with primers for *Il10rb* (Table S9).

Genotyping.

Genomic DNA was isolated from animal tissue using the hot-shot lysis procedure [33]. Genotyping PCR was carried out using *Taq*1 and gene-specific primer pairs (Table S9). For *Chaos3* genotyping, the PCR products were digested with MboII to identify mutant alleles as *Chaos3* but not wild-type alleles are digestible with this enzyme. For *Mcm5*, ES cells were verified using primers containing regions outside of the gene trap insertion to verify. To determine the sex of early embryos, primers for *Sry* (Sex-determining region Y) were used to identify males, females are *Sry* negative. Genotyping for *Mcm2–7* genetraps has been previously described [3].

Generation of *Mcm5* mutant mice.

Mcm5$^{tm1a(KOMP)Mbp}$ genetrap ES cells (Mcm5_F10, ESC#477873) were obtained from the Mouse Biology Program (MBP) at UC Davis and injected into B6(Cg)-*Tyr*$^{c-2J}$/*J* blastocyst donors to generate chimeras. Disruption of *Mcm5* was confirmed by PCR as described in genotyping section (Table S9). Following germline transmission, the mutation was backcrossed into C3H for ≥ 4 generations before crossing to C3H-*Mcm4*^{Chaos3} mice.

Generation of *FancM* mice.

Fancm$^{em1/Jcs}$ was generated using CRISPR/Cas9-mediated genome editing. In summary, an optimal guide sequence targeting the first exon of *Fancm* was designed using the mit.crispr.edu website. Oligos to generate the sgRNA DNA template were ordered from Integrated DNA Technologies (IDT) and the sgRNA was *in vitro* transcribed as described previously [34] (CRISPR-FancF: GAAATTAATACGACTCACTATAGGCCAGCTGGTAGTCGCGCACGGTTTTAGAGCTAGAAATAGC, CRISPR-FancR: CAAAATCTCGATCTTTATCGTTCAATTTTATTCCGATCAGGCAATAGTTGAACTTTTTCACCGTGGCTCAGCCACGAAAA). Embryo microinjection into C57BL/6J zygotes was performed as described previously [35] using 50ng/uL of sgRNA and 50ng/uL of Cas9 mRNA (TriLink Biotechnologies). The resulting 7bp deletion was identified via Sanger sequencing and subsequent genotyping was performed with primers sets specific to the mutant and wild-type alleles. (Table S9).

Flow cytometry to monitor X-inactivation.

A transgenic mouse [36] containing an X-linked *EGFP* was crossed to *Mcm4*^{Chaos3} mice, and FACS analysis of embryos was carried out as described in that citation. *Mcm4*$^{C3/+}$ *Mcm2*$^{Gt/+}$ males bearing an ubiquitously-expressed *X*-linked *GFP* transgene were bred to *Mcm4*$^{C3/C3}$ females. E10.5 female embryos (littermates from 7 different pregnancies), all of

which must bear the *GFP* transgene, were genotyped, dispersed into single cells, and analyzed by flow cytometry to determine the fraction of GFP+ cells. Theoretical maximum of GFP-positive cells in controls is 50%.

Quantitative real-time reverse transcription-PCR (qRT-PCR).

RNA was isolated from cells using a kit per manufacturer's instructions (Zymo or Qiagen RNeasy). 500ng of RNA was reverse transcribed into cDNA using qScript (Quanta) and analyzed on an ABI7300 or a Bio-Rad CFX96 using the following primers and iTaq (Bio-Rad). All reactions were normalized to *Gapdh* and/or *Tbp*. Primer sequences are available in Table S10. *Il6, Ptgs2, Mcm2, Mcm3, Mcm4, Mcm5*.

RNA-seq.

Total RNA was isolated from E13.5 placentas by homogenizing placentas in RNA lysis buffer followed by column purification per manufacturers' instructions (Omega Biotech). RNA sample quality was confirmed by spectrophotometry (Nanodrop) to determine concentration and chemical purity (A260/230 and A260/280 ratios) and with a Fragment Analyzer (Advanced Analytical) to determine RNA integrity. Ribosomal RNA was subtracted by hybridization from total RNA samples using the RiboZero Magnetic Gold H/M/R Kit (Illumina). Following cleanup by precipitation, rRNA-subtracted samples were quantified with a Qubit 2.0 (RNA HS kit; Thermo Fisher). TruSeq-barcoded RNAseq libraries were generated with the NEBNext Ultra II Directional RNA Library Prep Kit (New England Biolabs). Each library was be quantified with a Qubit 2.0 (dsDNA HS kit; Thermo Fisher) and the size distribution was be determined with a Fragment Analyzer (Advanced Analytical) prior to pooling. Libraries will be sequenced on a NextSeq500 instrument (Illumina). At least 20M single-end 75bp reads were generated per library. For analysis, reads were trimmed for low quality and adaptor sequences with cutadapt v1.8 using parameters: -m 50 -q 20 -a AGATCGGAAGAGCACACGTCTGAACTCCAG --match-read-wildcards. Reads were mapped to the mouse reference genome/transcriptome using tophat v2.1 with parameters: --library-type=fr-firststrand --no-novel-juncs -G <ref_genes.gtf>. For gene expression analysis: cufflinks v2.2 (cuffnorm/cuffdiff) was used to generate FPKM values and statistical analysis of differential gene expression [37]. For the GSEA analysis, all expressed genes were analyzed using the Hallmarks dataset [38]. The placental gene sets used were comparisons between male and female $Mcm4^{C3/C3}$ $Mcm2^{Gt/+}$ placentae from $Mcm4^{C3/C3}$ dams or $Mcm4^{C3/+}$ $Mcm2^{Gt/+}$ dams, and male versus female $Mcm4^{C3/C3}$ from $Mcm4^{C3/C3}$ dams.

Immunoblotting.

Protein was isolated from E13.5 placentas and embryos by acetone precipitation from RNA-isolation buffer (Buffer RLT or TRK) and resuspending in SUTEB loading buffer (8M Urea, 1% SDS, 10mM EDTA, 10mM Tris-HCl, pH 6.8). Protein lysates were run on 4–20% SDS-PAGE acrylamide gels and transferred to PVDF membrane (Millipore). Immunoblots were probed with anti-Mcm2 (Epitomics/Abcam), anti-MCM2(Cell Signaling Technology), anti-androgen receptor (Epitomics/Abcam), anti-SMAD2/3(Cell Signaling), anti-p21(Santa Cruz), anti-MCM4(Cell Signaling Technology), anti-actin (Sigma). Secondary antibodies used included goat anti-rabbit-HRP (Cell Signaling) and goat anti-mouse-HRP (Sigma).

Crescendo ECL substrate(Millipore) was used and immunoblots digitally scanned using a cDigit scanner. Quantification of immunoblots was performed using ImageStudio software.

γH2ax Staining.

Placentae from E13.5 embryos were dissected from individual embryos and washed in PBS. Decidua were separated from placenta and uterine tissue with fine forceps. Genotyping was carried out using a piece of the embryo. Placentae were flash-frozen in OCT and 10μM sections cut on a cryostat and affixed to slides. Sections were fixed for 10 minutes with 4% paraformaldehyde in PBS, and stained with mouse anti-γH2ax-phospho ser41 (Millipore) using a M.O.M kit and Biotin-Streptavidin blocking kit (Vector Labs) according to manufacturer's instructions. Alexa-488 or Alexa 647-streptavidin (Invitrogen) was used to visualize. Slides were scanned using a Scanscope FL with a 20X objective. Images were quantified using Fiji or HALO(Indica Labs) and foci were detected as described [39] with an added size parameter to differentiate between nuclei and cytoplasmic signals [40]

Hydroxyurea and IR treatment of embryos.

For irradiation experiments, pregnant females were irradiated with 5 Rads (50mGy), 3 times a week during gestation, beginning at E1.5. For HU experiments, hydroxyurea (Sigma) was dissolved at 10mg/ml in sterile 1X PBS for injection. Pregnant C3H females were subjected to daily i.p. injections of 30–50ug/kg beginning at E3.5. Control females received daily i.p injections of sterile 1X PBS alone. All pregnancies were carried to term and the number and sex of animals determined at birth.

Data Availability.

All data underlying the findings of this study are presented in the paper, except for RNA-seq data, which has been deposited into the GEO database (accession number GSE119710). Note that a source data file is online for the γH2AX and MCM protein quantifications.

Extended Data

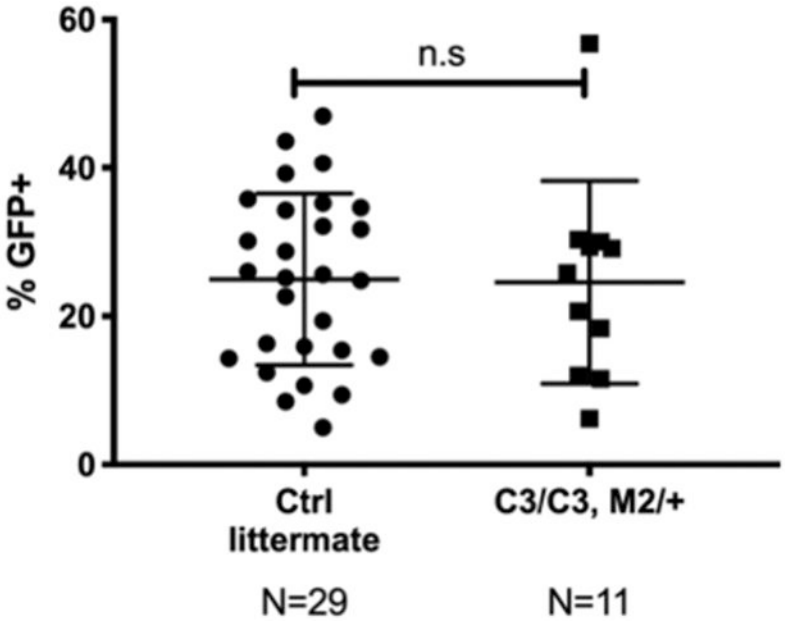

Extended Data Fig. 1. X-inactivation is not perturbed in MCM mutant embryos.

Mouse female embryos bearing one X-linked GFP transgene were dispersed into single cells and examined by flow cytometry for GFP fluorescence. Control animals were female littermates with a genotype of *Mcm4*$^{C3/+}$ *Mcm2*$^{+/+}$ or *Mcm4*$^{C3/C3}$ *Mcm2*$^{+/+}$. The center line represents the mean, and error bars represent the standard deviation in GFP-positive cells among the individual embryos (N) used. There is no significance difference between the values by an unpaired 2-tailed T-test(P=0.926). C3 = *Mcm4*^{Chaos3}; M2 = *Mcm2*^{Gt}.

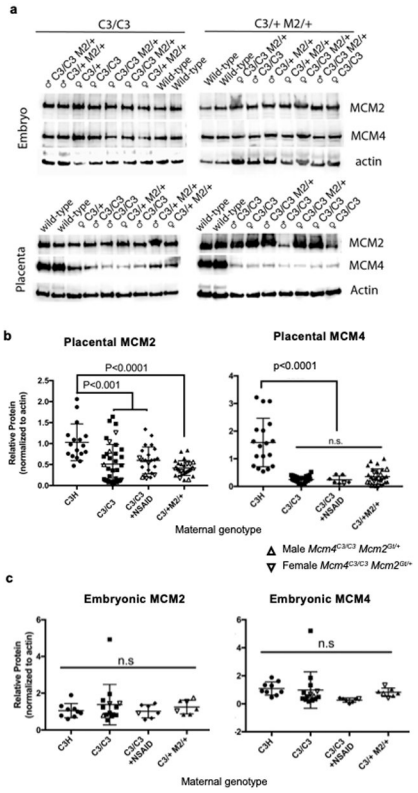

Extended Data Fig 2. Placental, but not embryonic MCM levels are decreased in MCM mutants independent of maternal genotype, and NSAID does not rescue MCM levels.

a) Representative westerns blots of protein lysates from E13.5 embryos and placentas of the indicated genotypes (top of each lane) were immunolabeled with antibodies against MCM2, MCM4, and beta actin. The samples came from dams of two genotypes indicated at the top of the panel. C3 = *Mcm4*^{Chaos3}; M2 = *Mcm2*^{Gt}. Note that MCM4 levels are particularly affected. The experiment was repeated twice for each maternal genotype. For gel source data, see Supplementary Figure 1. **b)** Placental MCM2 and MCM4 protein levels from the indicated maternal genotypes were quantified from western blots (including some other than those in "a") that were imaged (see Methods) and normalized to actin and WT protein levels. Each plotted point represents a single placenta. P-values represent unpaired two-tailed T-test. Placentae corresponding to male or female *Mcm4*$^{C3/C3}$ *Mcm2*$^{Gt/+}$ genotype are indicated. Centre values represent the mean and error bars indicate standard deviation. **c)** Embryonic MCM2 and MCM4 protein levels were determined as in (b). Each plotted point represents a single embryo. Embryos corresponding to male or female *Mcm4*$^{C3/C3}$ *Mcm2*$^{Gt/+}$ genotype are indicated. The results were not significant (n.s.) by a one-way ANOVA.

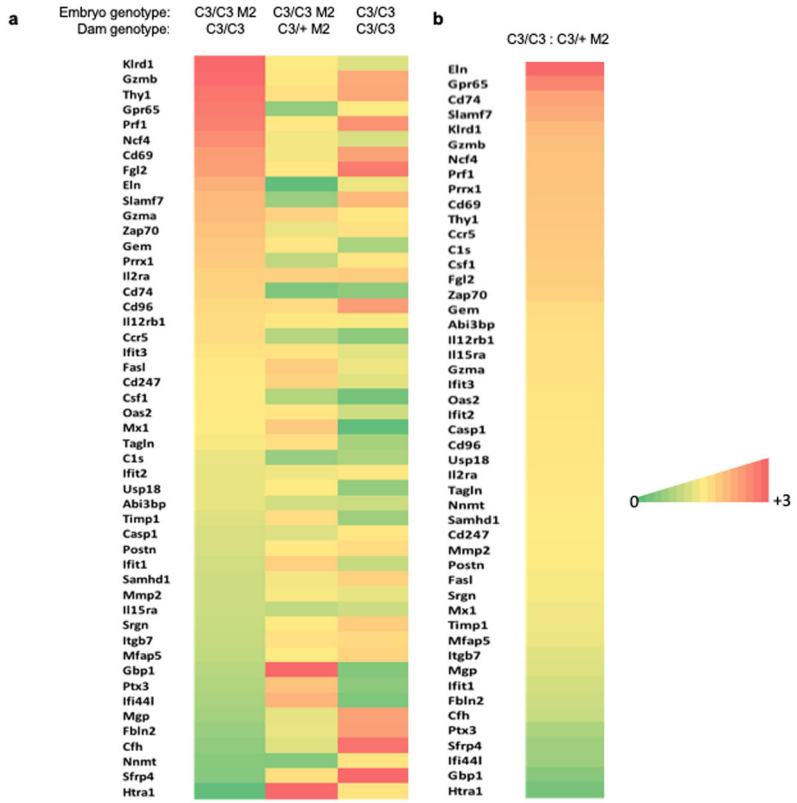

Extended Data Fig 3. Sex specific altered expression of inflammation genes in mutants.

a) Heatmap of the ratio of FPKM of key genes from top ranking genes from the following 3 GSEA Hallmarks: EMT, allograft rejection, and interferon gamma response. The ratios are expressed as female:male for each of the indicated embryo and dam genotypes. Data is from RNA-seq on n=16 placentas; n=6 *Mcm4*$^{C3/C3}$ *Mcm2*$^{Gt/+}$ from *Mcm4*$^{C3/C3}$ dams, n=6 from *Mcm4*$^{C3/+}$ *Mcm2*$^{Gt/+}$ dams, and n=4 from homozygous *Mcm4*$^{C3/C3}$ matings. Equal numbers of male and females were used. C3 = *Mcm4*^{C3}; M2 = *Mcm2*$^{Gt/+}$. **b)** Maternal genotype affects the expression of inflammation genes. Plotted are the female:male FPKM values of C3/C3 M2/+ embryos for C3/C3 dams compared to C3/+ M2 dams for the same gene sets as in (a). The highest and lowest genes are all related to inflammation responses.

Extended Data Table 1.

Segregation of genotypes from crosses.

a) Embryonic semilethality caused by the *Mcm4*$^{C3/C3}$ *Mcm2*$^{Gt/+}$ genotype is rescued by ibuprofen treatment of pregnant females. Cross: ♀ *Mcm4*$^{C3/C3}$ X ♂ *Mcm4*$^{C3/+}$ *Mcm2*$^{Gt/+}$. Red numbers are plotted in Fig. 2A under "NSAID." C3 = Chaos3. Data are from 29 litters. **b)** Embryonic semilethality caused by the *Mcm4*$^{C3/C3}$ *Mcm2*$^{Gt/+}$ genotype is affected by maternal genotype. Cross: ♀ *Mcm4*$^{C3/+}$ *Mcm2*$^{Gt/+}$ X ♂ *Mcm4*$^{C3/C3}$ Red numbers are plotted in Fig. 3A under "C3/+ M2/+." C3 = Chaos3, M2= Mcm2. Data are from 32 litters. **c)** Embryonic semilethality caused by the *Mcm4*$^{C3/C3}$ *Il10rb*$^{-/-}$ genotype is rescued by ibuprofen treatment of pregnant females. Cross: ♀ *Mcm4*$^{C3/C3}$ *Il10rb*$^{+/-}$ X ♂ *Mcm4*$^{C3/C3}$ *Il10rb*$^{+/-}$. **d)** Embryonic semi-lethality and female sex bias caused by the *FancM*$^{em1Jcs/em1Jcs}$ genotype (is rescued by ibuprofen treatment of pregnant females.) Cross: ♀ *Fancm*$^{em1Jcs/+}$ X ♂ *Fancm*$^{em1Jcs/+}$. Red numbers are plotted in Fig. 2A.

a

	Mcm4$^{C3/+}$	*Mcm4*$^{C3/+}$ *Mcm2*$^{Gt/+}$	*Mcm4*$^{C3/C3}$	*Mcm4*$^{C3/C3}$ *Mcm2*$^{Gt/+}$	Total
Males	29	38	21	14	102
Females	17	38	26	14	95
Total	46	76	47	28	197
%Female	36.9	50	55.3	50	48.2

b

	Mcm4$^{C3/+}$	*Mcm4*$^{C3/+}$ *Mcm2*$^{Gt/+}$	*Mcm4*$^{C3/C3}$	*Mcm4*$^{C3/C3}$ *Mcm2*$^{Gt/+}$	Total
Males	31	39	29	10	109
Females	25	38	17	14	94
Total	56	77	46	24	203
%Female	44.6	49.4	36.9	58.3	46.3

c

	Mcm4$^{C3/C3}$ *Il10rb*$^{-/-}$	*Mcm4*$^{C3/C3}$ *Il10rb*$^{+/-}$	*Mcm4*$^{C3/C3}$ *Il10rb*$^{+/+}$	Total
Males	1	15	3	19
Females	0	17	9	26
Total	1	32	12	45
%Female	0	53.5	75	58
		+NSAID		
Males	7	16	5	28
Females	9	21	10	40
Total	16	37	15	68
%Female	56	57	67	59

d

	Fancm$^{-/-}$	*Fancm*$^{+/-}$	+/+	Total
Males	32	70	34	136
Females	19	63	32	114
Total	51	133	66	250
%Female	37	47	48	46
		+NSAID		
Males	27	49	29	105
Females	24	43	27	94
Total	51	92	56	199
%Female	47	47	48	47

Supplementary Material

Refer to Web version on PubMed Central for supplementary material.

Acknowledgements.

We thank the Cornell Transgenic Core facility for help in producing the *Fancm* mutant mutant mice, and Jen Grenier from the RNA sequencing-seq Core. This work was supported by grants from NIH (R01 HD086609 and T32 HD057854 to JCS, the latter supporting MDW and JCB) and the Department of Defense (BC083376 to C-HC).

References

1. Rodier F et al. Persistent DNA damage signalling triggers senescence-associated inflammatory cytokine secretion. Nat. Cell Biol 11, 973–979 (2009). [PubMed: 19597488]
2. Nyberg KA, Michelson RJ, Putnam CW & Weinert TA Toward maintaining the genome: DNA damage and replication checkpoints. Annu. Rev. Genet 36, 617–656 (2002). [PubMed: 12429704]
3. Chuang C-H, Wallace MD, Abratte C, Southard T & Schimenti JC Incremental genetic perturbations to MCM2–7 expression and subcellular distribution reveal exquisite sensitivity of mice to DNA replication stress. PLoS Genet. 6, e1001110 (2010). [PubMed: 20838603]
4. Shima N et al. A viable allele of Mcm4 causes chromosome instability and mammary adenocarcinomas in mice. Nat. Genet 39, 93–98 (2007). [PubMed: 17143284]
5. Bianchi VE The Anti-Inflammatory Effects of Testosterone. Journal of the Endocrine Society 3, 91–107 (2019). [PubMed: 30582096]
6. Luo Y et al. Hypersensitivity of primordial germ cells to compromised replication-associated DNA repair involves ATM-p53-p21 signaling. PLoS Genet. 10, e1004471 (2014). [PubMed: 25010009]
7. Hills SA & Diffley JFX DNA replication and oncogene-induced replicative stress. Curr. Biol 24, R435–44 (2014). [PubMed: 24845676]
8. Zeman MK & Cimprich KA Causes and consequences of replication stress. Nat. Cell Biol 16, 2–9 (2014). [PubMed: 24366029]
9. Kato K, Omura H, Ishitani R & Nureki O Cyclic GMP-AMP as an Endogenous Second Messenger in Innate Immune Signaling by Cytosolic DNA. Annu. Rev. Biochem 86, 541–566 (2017). [PubMed: 28399655]
10. Yang H, Wang H, Ren J, Chen Q & Chen ZJ cGAS is essential for cellular senescence. Proc. Natl. Acad. Sci. USA 114, E4612–E4620 (2017). [PubMed: 28533362]
11. Ibarra A, Schwob E & Méndez J Excess MCM proteins protect human cells from replicative stress by licensing backup origins of replication. Proc. Natl. Acad. Sci. USA 105, 8956–8961 (2008). [PubMed: 18579778]
12. Woodward AM et al. Excess Mcm2–7 license dormant origins of replication that can be used under conditions of replicative stress. J. Cell Biol 173, 673–683 (2006). [PubMed: 16754955]
13. Ge XQ, Jackson DA & Blow JJ Dormant origins licensed by excess Mcm2–7 are required for human cells to survive replicative stress. Genes Dev. 21, 3331–3341 (2007). [PubMed: 18079179]
14. Kunnev D et al. DNA damage response and tumorigenesis in Mcm2-deficient mice. Oncogene 29, 3630–3638 (2010). [PubMed: 20440269]
15. Kawabata T et al. Stalled fork rescue via dormant replication origins in unchallenged S phase promotes proper chromosome segregation and tumor suppression. Mol. Cell 41, 543–553 (2011). [PubMed: 21362550]
16. Gondos B in Testicular Development, Structure and Function (eds. Steinberger A & Steinberger B) 3–20 (Raven Press, NY, 1980).
17. Litvinov IV et al. Androgen receptor as a licensing factor for DNA replication in androgen-sensitive prostate cancer cells. Proc. Natl. Acad. Sci. USA 103, 15085–15090 (2006). [PubMed: 17015840]
18. Shi Y-K et al. MCM7 interacts with androgen receptor. Am. J. Pathol 173, 1758–1767 (2008). [PubMed: 18988800]

19. Mackenzie KJ et al. cGAS surveillance of micronuclei links genome instability to innate immunity. Nature 548, 461–465 (2017). [PubMed: 28738408]
20. Liva SM & Voskuhl RR Testosterone acts directly on CD4+ T lymphocytes to increase IL-10 production. J. Immunol 167, 2060–2067 (2001). [PubMed: 11489988]
21. Malkin CJ et al. The effect of testosterone replacement on endogenous inflammatory cytokines and lipid profiles in hypogonadal men. J. Clin. Endocrinol. Metab 89, 3313–3318 (2004). [PubMed: 15240608]
22. Grosse A, Bartsch S & Baniahmad A Androgen receptor-mediated gene repression. Mol. Cell. Endocrinol 352, 46–56 (2012). [PubMed: 21784131]
23. Palayoor ST et al. Gene expression profile of coronary artery cells treated with nonsteroidal anti-inflammatory drugs reveals off-target effects. J. Cardiovasc. Pharmacol 59, 487–499 (2012). [PubMed: 22668799]
24. MacKenzie KF et al. MSK1 and MSK2 inhibit lipopolysaccharide-induced prostaglandin production via an interleukin-10 feedback loop. Mol. Cell. Biol 33, 1456–1467 (2013). [PubMed: 23382072]
25. Ahn J, Son S, Oliveira SC & Barber GN STING-Dependent Signaling Underlies IL-10 Controlled Inflammatory Colitis. Cell Rep. 21, 3873–3884 (2017). [PubMed: 29281834]
26. Cadet P, Rady PL, Tyring SK, Yandell RB & Hughes TK Interleukin-10 messenger ribonucleic acid in human placenta: implications of a role for interleukin-10 in fetal allograft protection. Am. J. Obstet. Gynecol 173, 25–29 (1995). [PubMed: 7631699]
27. Bai G, Smolka MB & Schimenti JC Chronic DNA Replication Stress Reduces Replicative Lifespan of Cells by TRP53-Dependent, microRNA-Assisted MCM2–7 Downregulation. PLoS Genet. 12, e1005787 (2016). [PubMed: 26765334]
28. Chuang C-H et al. Post-transcriptional homeostasis and regulation of MCM2–7 in mammalian cells. Nucleic Acids Res. 40, 4914–4924 (2012). [PubMed: 22362746]
29. Suarez-Carmona M, Lesage J, Cataldo D & Gilles C EMT and inflammation: inseparable actors of cancer progression. Mol. Oncol 11, 805–823 (2017). [PubMed: 28599100]
30. Bakker ST et al. Fancm-deficient mice reveal unique features of Fanconi anemia complementation group M. Hum. Mol. Genet 18, 3484–3495 (2009). [PubMed: 19561169]
31. Wolf CJ, Hotchkiss A, Ostby JS, LeBlanc GA & Gray LE Effects of prenatal testosterone propionate on the sexual development of male and female rats: a dose-response study. Toxicol. Sci 65, 71–86 (2002). [PubMed: 11752687]
32. Eicher EM, Shown EP & Washburn LL Sex reversal in C57BL/6J-YPOS mice corrected by a Sry transgene. Philos. Trans. R. Soc. Lond. B, Biol. Sci 350, 263–8; discussion 268 (1995). [PubMed: 8570690]
33. Truett GE et al. Preparation of PCR-quality mouse genomic DNA with hot sodium hydroxide and tris (HotSHOT). BioTechniques 29, 52–54 (2000). [PubMed: 10907076]
34. Varshney GK et al. High-throughput gene targeting and phenotyping in zebrafish using CRISPR/Cas9. Genome Res. 25, 1030–1042 (2015). [PubMed: 26048245]
35. Singh P, Schimenti JC & Bolcun-Filas E A mouse geneticist's practical guide to CRISPR applications. Genetics 199, 1–15 (2015). [PubMed: 25271304]
36. Hadjantonakis AK, Cox LL, Tam PP & Nagy A An X-linked GFP transgene reveals unexpected paternal X-chromosome activity in trophoblastic giant cells of the mouse placenta. Genesis 29, 133–140 (2001). [PubMed: 11252054]
37. Trapnell C et al. Transcript assembly and quantification by RNA-Seq reveals unannotated transcripts and isoform switching during cell differentiation. Nat. Biotechnol 28, 511–515 (2010). [PubMed: 20436464]
38. Subramanian A et al. Gene set enrichment analysis: a knowledge-based approach for interpreting genome-wide expression profiles. Proc. Natl. Acad. Sci. USA 102, 15545–15550 (2005). [PubMed: 16199517]
39. Rinaldi VD, Bloom JC & Schimenti JC Whole mount immunofluorescence and follicle quantification of cultured mouse ovaries. J. Vis. Exp. (2018). doi:10.3791/57593
40. Schindelin J et al. Fiji: an open-source platform for biological-image analysis. Nat. Methods 9, 676–682 (2012). [PubMed: 22743772]

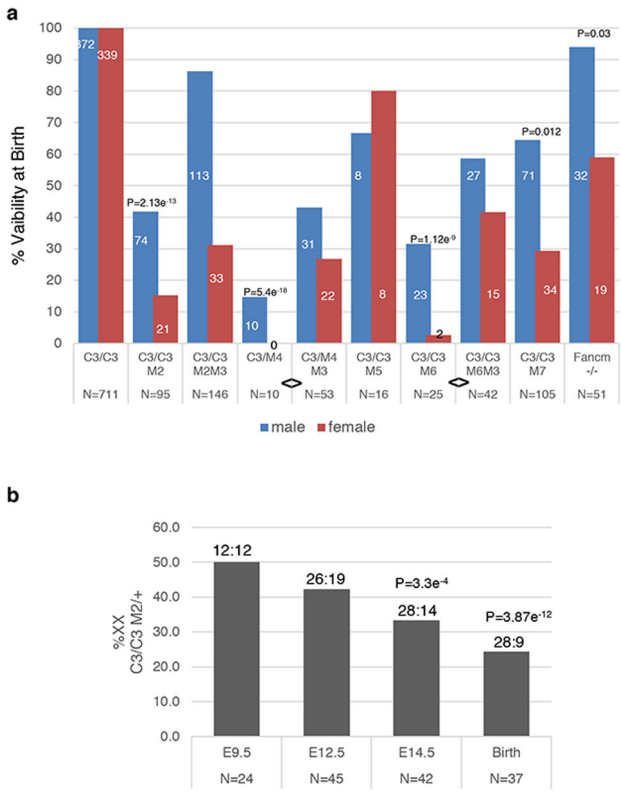

Fig. 1. Female-biased embryonic lethality in MCM-depleted mice.

(a) Female MCM-depleted mice are underrepresented at birth. Mice were bred to produce $Mcm4^{C3/C3}$ ("C3/C3") or $Mcm4^{Chaos3/Gt}$ offspring ("C3/M4), some of which were heterozygous for null alleles in other MCMs ("M#"; for example, M2/+ = $Mcm2^{Gt/+}$). Graphed are percent viability at birth of males and females for each of the indicated genotypes versus C3/C3 littermates. For *Fancm*, the viability is versus WT littermates. The numbers on or over the bars = # males or females of the indicated genotype, and the N values below equal the total number of newborns with that genotype. Some of the data for all genotypes except that involving M5 were reported in [3], but broken out by sex here and with added data that are enumerated in Extended Data Table 1 and Tables S1-S5. P-values are from a Chi-Squared test that females are underrepresented vs males from that genotype. "<>" represents a significant two-sided Fisher Exact Test (C3/M4; P=0.011, C3/M6; P=0.018) between indicated groups in terms of the ability of *Mcm3* heterozygosity to decrease sex bias. **(b)** Timing of female death during embryogenesis. E = embryonic day. Numbers above bars are viable XY:XX embryos genotyped (they sum to the "N" values). P-values determined from Chi-Squared probability.

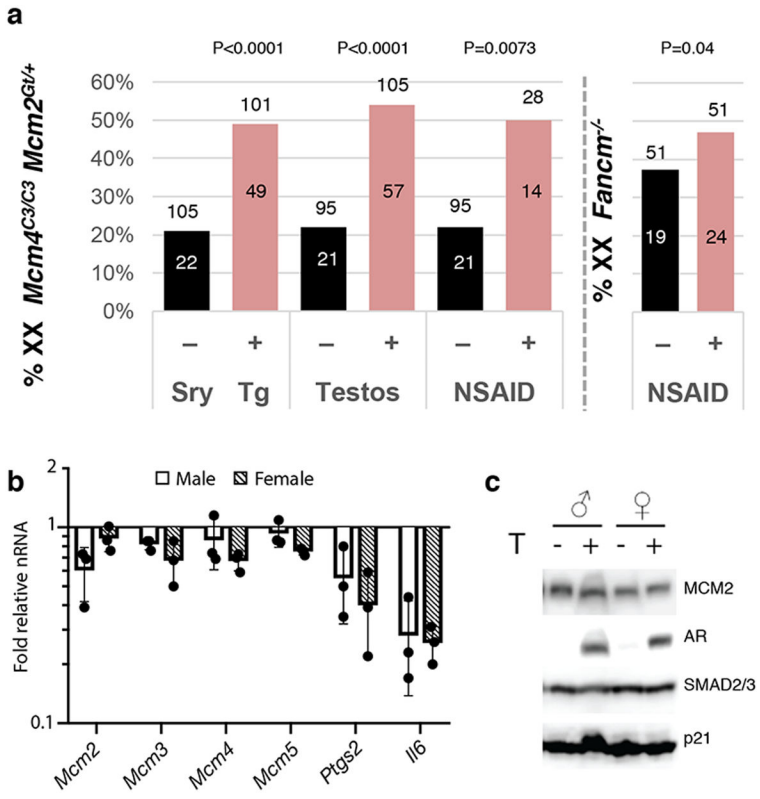

Fig. 2. Evidence that the anti-inflammatory activity of testosterone protects male embryos from genomic instability-induced lethality.

(a) Viability of genetically female (XX) *Mcm4*$^{C3/C3}$ *Mcm2*$^{Gt/+}$ or *Fancm*$^{-/-}$ embryos is rescued by *Sry* transgene-induced sex reversal (Sry Tg), and treatment of pregnant dams with either testosterone ("Testos") or ibuprofen ("NSAID"). Values above each bar are total mice, and those inside bars are XX. Nontransgenics and transgenics in the Sry Tg experiment were from the same cross. The untreated mice in the testosterone and NSAID experiments are from Table S3 and also plotted in Fig. 1a. This aggregate value contains 8 male and 1 female *Mcm4*$^{C3/C3}$ *Mcm2*$^{Gt/+}$ offspring that were produced contemporaneous to the NSAID cohort. P values are from two-tailed F.E.T. or an unpaired, 2-tailed T-test. The Sry Tg and testosterone crosses involved an *Mcm3*^{Gt} allele that was included to boost viability (but not sex skewing, see Fig. 1a) of the lethal genotypes. **(b)** Testosterone treatment does not affect *Mcm* mRNA, but does lower the inflammation markers *Il6* and *Ptgs2*. *Mcm4*$^{C3/C3}$ *Mcm2*$^{Gt/+}$ MEFs (n=6: 3 male, 3 female) were treated with 10nM T for 1 hr, and mRNA collected 6 hrs later for qRT-PCR. Bars represent mean and error bars indicate standard deviation. Individual data points are indicated. **(c)** Same as (b), but protein was collected 24 hrs after T treatment, and Western analysis performed with indicated antibodies by stripping and re-probing the same blot. The experiment was repeated a minimum of 3 times with different MEF lines of the same genotype with similar results. For gel source data, see Supplemental Figure 1.

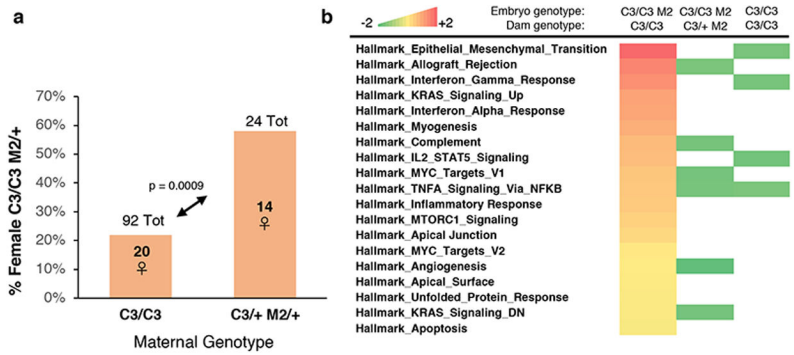

Fig 3. Maternal GIN genotype impacts female embryo viability and placental inflammation.

(a) Lethality of female (XX) *Mcm4*$^{C3/C3}$ *Mcm2*$^{Gt/+}$ embryos is dependent upon maternal genotype. C3 = *Mcm4*^{C3} ; M2 = *Mcm2*$^{Gt/+}$. Values above each bar are total mice, and those inside bars are XX. The P-value was calculated by a two-sided Fisher's Exact Test. See Tables S2 and Extended Data Table 1b for primary data from the crosses. **(b)** Placentae of female E13.5 embryos with the *Mcm4*$^{C3/C3}$ *Mcm2*$^{Gt/+}$ lethal genotype have elevated expression of inflammation pathways when the dam has elevated GIN. RNA-seq was carried out on n=16 placentae: n=6 *Mcm4*$^{C3/C3}$ *Mcm2*$^{Gt/+}$ from *Mcm4*$^{C3/C3}$ dams, n=6 from *Mcm4*$^{C3/+}$ *Mcm2*$^{Gt/+}$ dams, and n=4 from homozygous *Mcm4*$^{C3/C3}$ matings. Equal numbers of male and females were used. Shown are heatmaps of GSEA (Gene Set Enrichment Analysis) analysis of RNA-seq data, using the Hallmarks dataset of the Molecular Signatures Database (MSigDB; http://software.broadinstitute.org/gsea/msigdb/collections.jsp). Only those Hallmark pathways that were significantly different between sexes (FDR <0.25, nominal P value<0.05) were used to generate the heatmap. Multiple pathways involving inflammation are upregulated in *Mcm4*$^{C3/C3}$ *Mcm2*$^{Gt/+}$ female vs male embryos from *Mcm4*$^{C3/C3}$ dams, but not other combinations. Embryonic and maternal genotypes are listed at the top of the heatmaps.

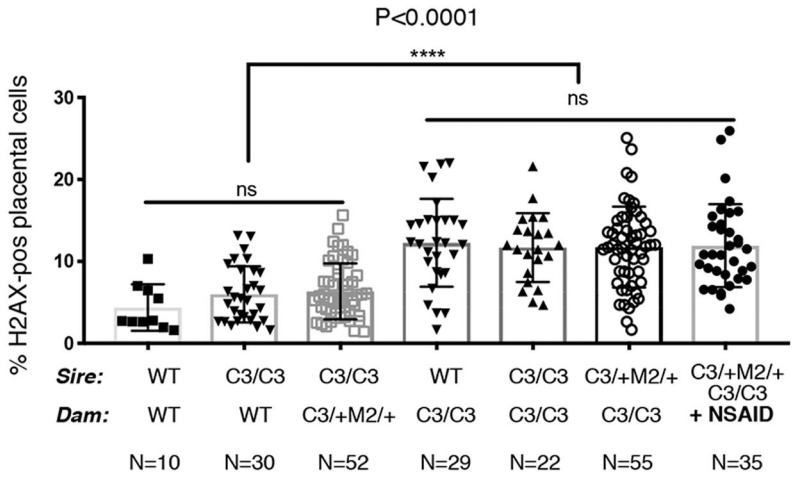

Fig. 4. Dams with intrinsic GIN cause elevated DNA damage in the placenta.

γH2AX staining in placentae from the indicated maternal genotypes. Each dot represents a single placenta. A minimum of 2 litters was examined per mating, total number of placentae analyzed is indicated. Significance was by unpaired, 2-tail t-tests. Centre value=mean, Error bars = standard deviation. ns = not significant.